Therapeutic potential of NTRK3 inhibition in desmoplastic small round cell tumor

Running title: NTRK3 as a therapeutic target in DSRCT

Koichi Ogura[1,2*], Romel Somwar[1,2*], Julija Hmeljak[1,2,*], Heather Magnan[3], Ryma Benayed[1], Amir Momeni Boroujeni[1], Anita S. Bowman[1], Marissa S. Mattar[4], Inna Khodos[4], Elisa de Stanchina[4], Achim Jungbluth[1], Marina Asher[1], Igor Odintsov[1,2], Alifiani B. Hartono[5], Michael P. LaQuaglia[3], Emily Slotkin[3], Christine A. Pratilas[6], Sean Bong Lee[5], Lee Spraggon[1,2,#], Marc Ladanyi[1,2,#]

[1]Department of Pathology, Memorial Sloan Kettering Cancer Center, New York, NY, USA
[2]Human Oncology and Pathogenesis Program, Memorial Sloan Kettering Cancer Center, New York, NY, USA
[3]Department of Pediatrics, Memorial Sloan Kettering Cancer Center, New York, NY, USA
[4]Anti-tumor Assessment Core Facility, Molecular Pharmacology Program, Memorial Sloan Kettering Cancer Center, New York, NY, USA
[5]Department of Pathology & Laboratory Medicine, Tulane University School of Medicine, New Orleans, LA, USA
[6]Division of Pediatric Oncology, Sidney Kimmel Comprehensive Cancer Center at Johns Hopkins, Baltimore, MD, USA

*These authors contributed equally to this study

[#] These authors share senior authorship.

Corresponding author: Marc Ladanyi, Department of Pathology, Memorial Sloan Kettering Cancer Center, 1275 York Ave, New York, NY, USA, 10065, ladanyim@mskcc.org

Key words: kinase signaling, desmoplastic small round cell tumor, entrectinib, patient derived xenografts

Conflict of interest disclosures

Romel Somwar has received research funding from LOXO Oncology, Helsinn Healthcare, Merus and Elevation Oncology to perform studies not related to this manuscript.

Marc Ladanyi has received advisory board compensation from Merck, Lilly Oncology, AstraZeneca, Bristol-Myers Squibb, Takeda, and Bayer, and research support from LOXO Oncology, Helsinn Healthcare, Elevation Oncology and Merus.

Christine A. Pratilas has received consulting fees from Genentech/ Roche; and receives research funding from Kura Oncology for studies not related to this manuscript.

Grant Support: Supported in part by the NCI Cancer Center Support Grant/Core Grant (P30 CA008748) and by NCI grant R01CA222856 (S.B.L).

Statement of Translational Relevance

Desmoplastic small round cell tumor (DSRCT) is an aggressive intra-abdominal sarcoma which arises primarily in adolescents and young adult (AYA) males, is defined by the *EWSR1-WT1* gene fusion, and has a 5-year survival of only 25% despite intensive multi-modality treatment. Identifying more effective, and molecularly selective, therapy is a clinical priority in this disease. Using a combinatorial approach of integrated and functional genomics, we identify NTRK3, a target of transcriptional activation by EWSR1-WT1, as a vulnerability that can be exploited for therapy for DSRCT. Targeting this receptor tyrosine kinase with entrectinib was sufficient to block growth of DSRCT cell lines and PDX tumors. Entrectinib is FDA-approved for use in the pediatric/AYA population for other indications and could therefore be quickly tested in clinical trials for DSRCT patients. Our results suggest that precision oncology is possible for pediatric sarcomas where the therapeutic target is transcriptionally rather than genetically altered, and that more efforts should be made to find new agents for the vast unmet need that currently exists in this class of sarcoma patients.

Abstract

Purpose: Desmoplastic small round cell tumor (DSRCT) is a highly lethal intra-abdominal sarcoma of adolescents and young adults. DSRCT harbors a t(11;22)(p13:q12) that generates the EWSR1-WT1 chimeric transcription factor, the key oncogenic driver of DSRCT. EWSR1-WT1 rewires global gene expression networks and activates aberrant expression of targets that together mediate oncogenesis. EWSR1-WT1 also activates a neural gene expression program.

Experimental Design: Among these neural markers, we find prominent expression of neurotrophic tyrosine kinase receptor 3 (NTRK3), a druggable receptor tyrosine kinase. We investigated the regulation of NTRK3 by EWSR1-WT1 and its potential as a therapeutic target *in vitro* and *in vivo,* the latter using novel patient-derived models of DSRCT.

Results: We find that EWSR1-WT1 binds upstream of *NTRK3* and activates its transcription. NTRK3 mRNA is highly expressed in DSRCT compared to other major chimeric transcription factor-driven sarcomas and most DSRCT are strongly immunoreactive for NTRK3 protein. Remarkably, expression of *NTRK3* kinase domain mRNA in DSRCT is also higher than in cancers with *NTRK3* fusions. Abrogation of NTRK3 expression by RNAi silencing reduces growth of DSRCT cells and pharmacologic targeting of NTRK3 with entrectinib is effective in both *in vitro* and *in vivo* models of DSRCT.

Conclusions: Our results indicate that EWSR1-WT1 directly activates NTRK3 expression in DSRCT cells, which are dependent on its expression and activity for growth. Pharmacologic inhibition of NTRK3 by entrectinib significantly reduces growth of DSRCT cells both *in vitro* and *in vivo*, providing a rationale for clinical evaluation of NTRK3 as a therapeutic target in DSRCT.

Introduction

First recognized as a clinicopathologic entity in 1989 by Gerald and Rosai, desmoplastic small round cell tumor (DSRCT) is an aggressive, primarily abdominal soft tissue sarcoma that affects mainly adolescents and young adults (1-3). Histologically, it is characterized by small round blue cells separated by abundant desmoplastic stroma and multilineage differentiation (2). Cytogenetic studies showed that DSRCT tumor samples contain a specific, reciprocal chromosomal translocation, t(11;22)(p13:q12) (4). In 1994, together with the Gerald laboratory, we showed that the t(11;22)(p13:q12) generates the *EWSR1-WT1* chimeric transcription factor (5,6) which fuses the transcriptional regulatory domain of *EWSR1* to the DNA-binding domain of *WT1*.

Therapy for DSRCT most often involves intensive multi-modality treatment with chemotherapy, surgery, and radiotherapy, and sometimes, intraperitoneal infusions of chemotherapy or investigational radio-isotope labelled antibody such as 8H9 (7). Despite these aggressive measures, the overall 5-year survival for patients with this disease remains dismal, typically around 25%. Hence, new forms of therapy and therapeutic targets are urgently needed. EWSR1-WT1, the protein encoded by *EWSR1-WT1*, rewires global gene expression networks, modulating aberrant expression of targets that contribute to an oncogenic expression program. While a number of genes transcriptionally upregulated by EWSR1-WT1 have been identified (8-10), none have translated into promising therapeutic targets. More recently, we have demonstrated a broader involvement of EWSR1-WT1 in the regulation of neural gene expression (11), supporting the hypothesis that targeting neural differentiation markers might offer a novel arena in which to develop therapeutic approaches to treat DSRCT.

In the present study, we applied a combinatorial approach of integrated and functional genomics to identify therapeutic targets for the treatment for DSRCT. We report that *NTRK3* is a direct target of the EWSR-WT1 chimera and is highly expressed in DSRCT tumors. Pharmacological targeting of the NTRK signaling pathway is effective both in patient-derived *in vitro* and *in vivo* pre-clinical models of DSCRT.

n is active in recent publications of DSRCT (12,13).

Materials and Methods

Cell culture media, antibiotics and phosphate-buffered saline (PBS) were prepared by the MSK Media Preparation Core Facility. Fetal bovine serum (FBS) was procured from Atlanta Biologicals (Flowery Branch, GA). HEK-293T cells were obtained from American Type Culture Collection (Manassas, VA). The LP-9 cell line is an untransformed, diploid, mesothelial cell line that was derived from a 26-year old female ovarian cancer patient and was obtained from the Coriell Institute for Medical Research (Camden, NJ). Antibodies to native and/or phosphorylated proteins were purchased from Cell Signaling Technology (Boston, MA). Small molecule inhibitors were obtained from Selleckchem (Houston, TX). Promega's ApoOne Homogenous Caspase 3/7 activity assay kit, AlamarBlue, puromycin, geneticin, tissue culture plastic wares, TaqMan real-time PCR probes and all Western blotting reagents were obtained from ThermoFisher Scientific (Waltman, MA). Protease inhibitor cocktail, RIPA buffer (10X) and all other chemicals not listed above were purchased from EMD-Millipore Sigma (St. Louis, MO). All oligonucleotides used for PCR assays were obtained from Integrated DNA technologies (Coralville, IA). Recombinant human NTF3 Protein was obtained from R&D Systems Inc (Minneapolis, MN). Patient tumor samples were obtained under Memorial Sloan Kettering Cancer Center Institutional Review Board (IRB) protocols 06-107 and 12-245 as described previously (14).

Cell culture and reagents.

The cell lines were cultured in the recommended medium supplemented with 10% heat-inactivated fetal bovine serum (FBS) and penicillin-streptomycin in a 5% CO_2 humidified incubator at 37 °C.

For the growth curve analysis, cells were seeded in 6-well plate (20,000 cells per well) in DMEM:F12 growth medium supplemented with 2% FBS and 1% antibiotics. TaqMan real-time PCR probes were obtained from ThermoFisher Scientific (Waltham, MA).

RT-PCR

Total RNA was extracted from cells or frozen PDX tissues using the RNAqueous-Micro Total RNA Isolation kit (Ambion; Thermo Fisher Scientific, Waltham, MA, USA) and total RNA (200 ng) were reverse-transcribed into cDNA using SuperScript VILO cDNA Synthesis Master Mix (ThermoFisher Scientific).

cDNA was subjected to PCR amplification using AmpliTaq Gold 360 Master Mix (ThermoFisher Scientific, Waltham, MA). The reactions were carried out in a thermal cycler under the following conditions: 95°C for 5 min, 35 cycles of 95°C for 15 sec, 58°C for 30 sec, and 72°C for 1 min, with a final extension at 72°C for 10 min for *EWSR1-WT1*.

GAPDH was amplified to estimate the efficiency of cDNA synthesis under the following conditions: 95°C for 5 min, 33 cycles of 95°C for 15 sec, 60°C for 30 sec, and 72°C for 1 min, with a final extension at 72°C for 10 min. No-reverse transcriptase (− RT) and no-template (NTC) reactions were used as negative controls.

The PCR primers used in this study are as follows.

*EWSR1-WT1*fusion: F (5’ ACTGGATCCTACAGCCAAGCTC3’) (EWSR1 exon 7 forward) and R (5’ GCCACCGACAGCTGAAGGGCT3’) (WT1 exon 10 reverse)

GAPDH: F (5’ AAAGTTGTCATGGATGACCTTGG3’) and R (5’ GGCGCTGAGTACGTCGTGGAGTCCA3’)

Quantitative reverse transcription PCR (RT-qPCR)

RT-qPCR was performed using the TaqMan® Gene Expression Master Mix and 'inventoried' TaqMan® Gene Expression assays (Applied Biosystems, Foster City, CA), using standard reaction-mix setups and cycling protocol for a StepOne Real-Time PCR System (Applied Biosystems). Gene expression was quantified with the $\Delta\Delta C_T$ method, using *GAPDH* as an internal control. The TaqMan probes used are as follows: WT1 c terminal (Assay ID, PN4331348 or Hs01103755_m1), NTRK1 (Assay ID, Hs01021011_m1), NTRK2 (Assay ID, Hs00178811_m1), NTRK3 (Assay ID, Hs00176797_m1), NGF (Assay ID, Hs00171458_m1), BDNF (Assay ID, Hs02718934_s1), NTF3 (Assay ID, Hs00267375_s1), and GAPDH (Assay ID, Hs02758991_g1).

Immunohistochemistry

IHC staining for NTRK3 was performed with an N-terminal NTRK3 rabbit monoclonal antibody (clone C44H5) from Cell Signaling, at 1:100 dilution. All assays were performed on a Leica-Bond-3 (Leica, Buffalo Grove, IL) automated staining platform using a heat-based antigen retrieval method and high pH buffer solution (ER2, Leica).

Agilent ChIP-chip Arrays

We mined legacy ChIP-chip data that had been previously generated as follows. Genomic DNA was hybridized to the Agilent Human Promoter Array (Agilent Technologies). The ChIP assay was performed as described before (15) using anti-WT1 (C19; Santa Cruz Biotechnology) in the JN-DSRCT1 cell line which expresses endogenous EWSR1-WT1, but not native WT1, and using

anti-HA in the UF5 cell line (16), generated by introduction of a tetracycline-repressible cDNA encoding an HA-tagged EWSR1-WT1 (-KTS) in the UF5 osteosarcoma cell line.

Luciferase Reporter Assay

Exponentially growing HEK293T cells were co-transfected with either (HA)-EWSR1-WT1 (-KTS), (HA)-EWSR1-FLI1 or pcDNA3.1 expression constructs, and *Gaussia* Luciferase-fused *NTRK3* and *ASCL1* promoter pEZX-PG04 plasmids (Genecopeia). The reporter assay was performed using the Secrete-Pair Dual Luminescence Assay Kit (Genecopeia) according to the manufacturer's instructions. Briefly, 48 hours post-transfection, growth media was collected and transferred to a luminescence-compatible microtiter plate. Secreted luciferase activity was assayed on a BioTek luminometer with XYs integration. Secreted alkaline phosphatase was use for normalization. Luciferase and alkaline phosphatase measurements were performed in triplicates and all experiments were repeated at least twice. Expression levels of HA-EWSR1-WT1 and (HA)-EWSR1-FLI1 were assayed via western blot with a rabbit monoclonal anti-HA-tag antibody (Cell Signaling Technology).

Lysate preparation, IP, and immunoblotting

Cells were washed twice with ice cold PBS and lysed in 1x RIPA lysis buffer (Cell Signaling Technology, Danvers, MA) supplemented with Complete protease inhibitor cocktail (# 05892791001, Roche, Germany) and PhosSTOP (# 04906837001, Roche, Germany). The cells were solubilized by incubation for 30 min at 4°C on a shaking platform. The lysates were centrifuged at 14,000 xg, 4^{o}C for 10 min in a microcentrifuge. Protein quantification of the lysates was performed with a DC protein assay kit from Bio-Rad. Protein expression was

determined either via Western blot analysis or immunoprecipitation (IP) followed by Western blot analysis with anti-phosphor-tyrosine antibody. For Western blot analysis, 30 µg of total cell lysate was mixed with Laemmli buffer and resolved by SDS-PAGE.

IPs were performed on 1000 µg of total cell lysate with anti-NTRK3 antibody (1:50 dilution) and Pierce Protein A/G magnetic beads (Thermo Scientific) according to the manufacturer's protocol. After the final wash was removed from the beads, 40 µl of Laemmli buffer was added. The samples were boiled for 5 min before loading, and resolved on 4-12 % Bis-Tris mini gels (Nupage) by SDS-PAGE and transferred electrophoretically to nitrocellulose membrane. Blots were blocked with 5% non-fat milk in TBST for 1 h then incubated with primary antibody in 3% bovine serum albumin (BSA) overnight.

To confirm that JN-DSRCT-1 does not express native WT1, we used WT1 C-terminus antibody from ThermoFisher (# PA5-16879). TET-off inducible U2OS cell lines that express wildtype WT1 (UB27, WT1-KTS, and UD28, WT1+KTS) were used as controls (17).

Other antibodies used were against NTRK3 (1:1000 for immunoblotting and 1:50 for IP; #3376, Cell Signaling Technology), AKT (1:2000; # 4691, Cell Signaling Technology), p44/42 ERK (1:2000; # 4695, Cell Signaling Technology), phosphorylated AKT (Ser473) (1:2500; # 4060, Cell Signaling Technology), phosphorylated p44/42 ERK (Thr202/Tyr204) (1:2500; # 4370, Cell Signaling Technology), phospho-tyrosine (1:2000; # 9411, Cell Signaling Technology), and GAPDH (1:2500; # 2118, Cell Signaling Technology). Membranes were incubated for 1 hour with secondary anti-rabbit antibody (1:2500-1:7500, HRP-linked, # 7074, Cell Signaling Technology) or anti-mouse antibody (1:2500, HRP-linked, # 7076, Cell Signaling Technology) in 5% skim milk in TBST.

Establishment of patient-derived cell lines and xenografts, and efficacy studies

All mice were cared for in accordance with guidelines approved by the Memorial Sloan Kettering Cancer Center Institutional Animal Care and Use Committee and Research Animal Resource Center and animals were monitored daily. Tissue samples were collected under an institutional IRB-approved biospecimen collection protocol as described previously (14). The SK-DSRCT2 cell line was created from a surgically resected abdominal tumor which was cut into small pieces with a scalpel in serum-free DMEM:F12 growth media and then digested for 1 h with collagenase (2mg/mL) in final volume of 5 mL, at 37^{o}C. The sample was vortexed every 5 mins and then DMEM:F12+10% FBS media was added to a final volume of 50 mL, centrifuged to pellet cells and then plated in DMEM:F12 growth medium supplemented with 10% FBS and 1% antibiotics. The sample was allowed to propagate over multiple generations, trypsinized when necessary to subculture and eventually only single cells remained. Unless indicated otherwise, all cell lines were maintained in DMEM:F12 growth medium supplemented with 10% FBS and 1% antibiotics for experiments in a humidified incubator infused with 5% CO_2 and sub-cultured when the stock flasks reached approximately 75% confluence at a 1:3 dilution. To establish the PDX models, freshly collected tumor samples were cleaned and then minced, mixed with Matrigel and implanted subcutaneously in the flank of female *NOD/SCID* gamma (NSG, Jackson Laboratory #005557, Bar Harbor, ME) mice (18). For cell line xenografts, 10 million cells were mixed with Matrigel (1:1) and injected subcutaneously into a single flank of female NSG mice. When tumors reached approximately 80-100 mm^3 volume, mice were randomized into groups of 5, and treated with vehicle or entrectinib (50 mg/kg QD). Tumors size and body weight were measured twice weekly and tumor volume was calculated

using the formula: length x width^2 × 0.52. All mice were sacrificed before tumor-associated death when tumors reached a size of 1000-1500 mm^3, and treatment duration ranged 6-10 weeks.

Results

Identification of *NTRK3* as a direct transcriptional target of EWSR1-WT1

To identify direct targets of the EWSR1-WT1 transcription factor, we performed a genome-wide location analysis using chromatin immunoprecipitation (ChIP) in the JN-DSCRT-1 cell line, the only widely available DSRCT cell line. Notably, this cell line does not express native WT1 (Supplementary Figure 1) (wild type WT1 is typically not expressed in DSRCT (19,20), and therefore ChIP using a WT1 C-terminus antibody was effectively used to assay EWSR1-WT1 DNA binding. In addition, we performed similar experiments in UF5 cells, which were generated by introduction of a tetracycline-repressible cDNA encoding an HA-tagged transcriptionally active isoform of EWSR1-WT1 (-KTS) in the UF5 osteosarcoma cell line (16). We identified peak EWSR1-WT1 binding positions in 2324 and 2939 regions for anti-WT1 and anti-HA antibodies, in the JN-DSRCT1 and UF5 cells, respectively. Data from these two independent model systems were then cross referenced, in order to focus on the most specific and reproducible results. This yielded 1501 regions scoring positive for EWSR1-WT1 binding by both ChIP approaches (Figure 1A, Supplementary Table 1). Among these was *ASCL1*, a previously well characterized direct target of EWSR1-WT1 (11), confirming the validity of the approach.

Next, we triaged these 1501 putative EWSR1-WT1 targets against transcriptomic data obtained from expression profiling of the JN-DSRCT-1 and UF5 cell lines. This allowed us to pursue the candidates identified via ChIP whose expression was upregulated in the presence of the EWSR1-WT1 transcription factor. Assessing the list of candidates for direct targets of transcriptional upregulation by EWSR1-WT1, we then narrowed down our list to genes that are potentially druggable/actionable targets using the OncoKB database (21). From this list, we

identified 7 genes based on OncoKB Levels 1-3. (Supplementary Table 2) and focused our attention on *NTRK3*, which represents, when activated by gene fusion, a Level 1 target (FDA-recognized biomarker predictive of response to an FDA-approved drug in a tumor-type agnostic indication).

NTRK3 is a transmembrane receptor tyrosine kinase (RTK) belonging to the NTRK receptor family. This family consists of three transmembrane proteins referred to as NTRK1/TrkA, NTRK2/TrkB and NTRK3/TrkC receptors, and are encoded by the *NTRK1*, *NTRK2* and *NTRK3* genes, respectively. Predominantly involved in neuronal development, NTRK proteins play essential roles in both the development and function of the nervous system through neurotrophin (NT) signal transduction. Each NTRK receptor is activated by a distinct ligand, with NTF3 representing the ligand for NTRK3. Gene rearrangements involving NTRK1-3 have recently emerged as important targets for cancer therapy (22). We identified several EWSR1-WT1 binding regions in the regulatory region of *NTRK3* (Supplementary Table 1), suggesting that *NTRK3* could be a direct transcriptional target of EWSR1-WT1. Using ChIP-qPCR, we further validated this finding in JN-DSRCT-1 cells and a new DSRCT patient-derived cell line that we have developed, SK-DSRCT2 (confirmed to contain the *EWSR1-WT1* fusion by RT-PCR and FISH, see Supplementary Figure 2). An element located at 170bp from the transcriptional start site represented a *bona fide* binding site for EWSR1-WT1, with 14- and 5-fold enrichment in the *NTRK3* promoter in JN-DSRCT-1 and SK-DSRCT2 cells, respectively. As a positive control, we also carried out a ChIP-qPCR assay for *ASCL1*, a previously validated EWSR1-WT1 transcriptional target (11), in both DSRCT cell lines and found a 7- and 12-fold enrichment, confirming the validity of our experimental approach (Figure 1B).

To confirm transcriptional activation of NTRK3 expression, we ectopically expressed the EWSR1-WT1 (-KTS) isoform, which is the more transcriptionally active isoform (6), in the human embryonic kidney cell line, HEK293T (Figure 1C, left panel). This resulted in potent induction of *NTRK3* mRNA as assayed by qRT-PCR, when compared to empty control expression vectors (Figure 1C, right panel). No changes in the level of mRNAs for *NTRK1*, *NTRK2* or *NTF3* (neurotrophin 3), the ligand for NTRK3, were detected (Figure 1C, right panel). Similar results were observed in the UF5 cell line, with expression of NTRK3 detected only in the presence of the EWSR1-WT1 (-KTS) isoform, and no induction of *NTF3* or other *NTRK* family members (Supplementary Figure 3).

Having identified an EWSR1-WT1 bound element in the *NTRK3* promoter and having found that ectopic expression of EWSR1-WT1 in heterologous cell lines induced robust expression of *NTRK3*, we next tested the proximal *NTRK3* promoter encompassing this element in a luciferase reporter assay to demonstrate direct transcriptional control of activation. Expression of EWSR1-WT1 (-KTS) in the HEK293T cell line in resulted in increased activity of the *NTRK3* promoter construct (Figure 1D), whereas expression of EWSR1-FLI1 had no effect. There was no activation of transcription of the *NTRK3* promoter construct using the EWSR1-WT1 (+KTS) isoform further supporting the specificity of the observation (data not shown). In support of these data, knockdown of EWSR1-WT1 with WT1 siRNA targeting the region retained in the fusion transcript resulted in a significant reduction in *NTRK3* mRNA in the JN-DSRCT1 cell line (Figure 1E). As expected (23), JN-DSRCT1 cells were dependent on EWSR1-WT1 expression for growth and survival, the latter measured by caspase activation (Figure 1E). In contrast, in the CHP100 Ewing sarcoma line, the same WT1 siRNA showed knockdown of native WT1 but no significant effects on NTRK3 expression, cell numbers, or

caspase activation (Figure 1E). Taken together, these data show that EWSR1-WT1 binds to the proximal promoter region of *NTRK3* and activates its expression.

NTRK3 is highly expressed in DSRCT

Having found that *NTRK3* is a direct target of EWSR1-WT1 in cell lines, we next assessed expression of *NTRK3* mRNA in DSRCT tumor samples and DSRCT cell lines. We compared the mRNA expression level of *NTRK3* across 137 tumor samples from four other major translocation sarcomas: Ewing sarcoma, alveolar rhabdomyosarcoma, synovial sarcoma and alveolar soft part sarcoma in legacy Affymetrix microarray data, of which the details are provided elsewhere(15,24). Expression of *NTRK3* mRNA in DSRCT was significantly higher than in these other translocation positive sarcomas ($P < 0.001$) (Figure 2A). To further characterize the level of NTRK expression in DSRCT patient samples, we analyzed data generated by the MSK-Fusion clinical assay (25), which is based on anchored RT-PCR and includes primers for exons encoding the NTRK3 kinase domain. The expression of *NTRK3* kinase domain mRNA was higher in DSRCT cases compared to non-DSRCT clinical solid tumor samples, including, remarkably, cancers with *NTRK3* fusions (Figure 2B). We also examined NTRK3 protein expression in DSRCT tumor samples using IHC. DSRCT samples stained strongly for NTRK3 in contrast to the surrounding stroma which was negative (Figure 2C). Finally, in a separate genomic profiling study of DSRCT tumor samples from 52 patients analyzed using the MSK-IMPACT assay, all samples had wildtype *NTRK3* (26), ruling out the possibility that NTRK3 overexpression in DSRCT is associated with mutation or rearrangement of *NTRK3*. Taken together, these data indicate that wild type NTRK3 is highly and consistently expressed in DSRCT tumors.

NTRK3 signaling is active in DSRCT cell lines and regulates growth

To better understand the functional status of NTRK3 in DSRCT, we examined expression of *NTRK* and *NTF* isoforms in patient-derived DSRCT cell lines (Figure 3A) by qPCR. NTRK3 and its ligand NTF3 were highly expressed at the mRNA level in JN-DSRCT-1 and SK-DSRCT2 cell lines but not in LP9, a non-transformed mesothelial cell line derived from the peritoneum, or in CHP100, a Ewing sarcoma cell line expressing the *EWSR1-FLI1* fusion (Figure 3A). NTRK3 and NTF3 proteins were confirmed to be highly expressed by Western blotting mainly in DSRCT cell lines (Figure 3B). Expression of EWSR1-WT1, as assayed by a C-terminal antibody to WT1, mirrored that of NTRK3 and NTF3 (Figure 3B).

To determine if NTRK3 signaling is active in DSRCT cells, we next looked at NTRK3 phosphorylation by IP-Western. This showed that NTRK3 is phosphorylated on tyrosine residues in JN-DSRCT-1 cells. No detectable phosphorylation was detected in CHP100 cells (Figure 3C). Treatment of DSRCT cell lines with NTF3 caused a dose-dependent increase in phosphorylation of ERK, a key mediator of mitogenic signaling (Figure 3D). Accordingly, treatment of DSRCT cell lines with NTF3 also caused a significant increase in cell growth (Figure 3E).

To determine if NTRK3 is required for growth of DSRCT cells, we treated cells with the pan-NTRK inhibitor entrectinib, recently approved by the US FDA for the treatment of cancers with *NTRK* fusions. Treatment of DSRCT cells with entrectinib reduced phosphorylation of ERK (Figure 4A) and inhibited their growth more potently than that of CHP100 or LP9 cells (Figure 4B-C). Growth of DSRCT cell lines was also reduced by repotrectinib, another kinase inhibitor with anti-NTRK activity (27) (Figure 4D), accompanied by decreased phosphorylation

of ERK (Figure 4E). Notably, other targets of entrectinib (and repotrectinib), such as ALK and ROS1, are not expressed in DSRCT (Supplementary Figure 4) (28).

To ensure that inhibition of NTRK3 by entrectinib and repotrectinib was responsible for the reduced viability, we knocked down NTRK3 using two shRNAs which were confirmed to be effective in JN-DSRCT-1, SK-DSRCT-2 and CHP100 cells (Figure 5A-C). However, viability was only reduced in the two DSRCT cell lines, suggesting that NTRK3 is required for growth of DSRCT cells specifically (Figure 5A-C). As we observed with entrectinib, RNA interference-mediated inhibition of NTRK3 also leads to loss of ERK phosphorylation (Figure 5D). Thus, both pharmacologic and genetic targeting support a dependence of mitogenic signaling and growth in DSRCT cells on NTRK3.

Entrectinib effectively reduces growth of DSRCT *in vivo*.

To examine *in vivo* if this dependence of DSRCT cell on NTRK3 can be exploited for therapy, we developed three novel DSRCT PDXs (Supplementary Table 3). RT-PCR confirmed that the PDX tumors express the *EWSR1-WT1* fusion mRNA (Figure 6A) as well as high levels of *NTRK3* and *NTF3* (Figure 6B). We next treated mice bearing these three DSRCT PDX models with the orally bioavailable small molecule NTRK3 inhibitor entrectinib. Animals were treated once daily with 30 mg/kg entrectinib on a schedule of 5 days on / 2 days off. Tumor growth is shown in Figure 6C-E). We used the area under curve analysis (AUC) to compare the effect of treatment between the two groups as this analysis takes into account the magnitude and duration of the treatment effect. Entrectinib treatment significantly reduced growth of all three DSRCT PDX models. Growth of DSRCT-0024Bpdx tumors was inhibited almost completely, whereas entrectinib inhibited growth of DSRCT-0027Apdx tumors and DSCT-0016Apdx tumors by

approximately 75 and 50%, respectively. Possibly, the lesser inhibition in the latter two models may reflect concurrent activation of other RTKs by EWSR1-WT1 in these cases (29), or may represent the effect of concomitant mutations. Western blot analysis of DSRCT-0027A PDX tumor samples obtained at time of sacrifice confirmed that entrectinib reduced ERK signaling downstream of NTRK3 (Figure 6F). Finally, entrectinib therapy was well tolerated and did not cause any significant change in animal body weight (Figure 6C-E, inset).

Discussion

Desmoplastic small round cell tumor (DSRCT) is an aggressive intra-abdominal sarcoma which arises primarily in adolescents and young adult (AYA) males, is defined by the *EWSR1-WT1* gene fusion, and has a 5 year survival of only 25% despite intensive multi-modality treatment. Unlike many other tumor types, cancers driven by chimeric transcription factors resulting from chromosomal translocations rarely harbor currently targetable genetic alterations. In this class of tumors, the promise of prospective clinical genomic profiling has not yet translated into clinical advances. However, chimeric transcription factors may promote cell proliferation through the transcriptional activation of various mitogenic signaling pathways. Targeting these may provide a therapeutic opportunity in this relatively "undruggable" class of cancers (30-32). Here, we show that transcriptional activation of the NTRK3 RTK by EWSR1-WT1 plays a major role in the biology and proliferative activity of DSRCT. As NTRK3 is targetable by highly potent new pan-NTRK inhibitors, its expression creates a novel therapeutic opportunity in this aggressive, highly lethal pediatric/young adult soft tissue sarcoma.

NTRK kinase inhibition by a new generation of highly potent NTRK inhibitors has emerged as a viable treatment option for patients with tumors carrying *NTRK* gene fusions as demonstrated by its *in vitro* and *in vivo* anti-tumor efficacy in multiple preclinical *NTRK* fusion-bearing tumor models (33-36), and by the robust clinical responses in patients with *NTRK*-rearranged tumors observed across a broad range of solid tumors (37). Given the clinical successes of NTRK inhibition by entrectinib, we hypothesized that pan-NTRK inhibitors should reduce the growth of DSRCT tumors. Indeed, NTRK inhibition *in vitro* by entrectinib and repotrectinib decreased NTRK3 mRNA expression, blocked NTRK3 downstream signaling and suppressed cell proliferation. Our *in vivo* studies were facilitated by the development of a new cell line and three new PDX models. Using these new *in vitro* and *in vivo* models, we have generated preclinical data that provide a rationale for clinical evaluation of NTRK3 inhibitors in patients with DSRCT. Although our preclinical studies did not test NTRK3 inhibitors in combination with existing agents, they do provide a further impetus for the opening of a previously planned clinical trial evaluating the NTRK inhibitor, repotrectinib, in combination with irinotecan and temozolomide in children and young adults with relapsed or refractory DSRCT at Memorial Sloan Kettering Cancer Center. The decision to combine repotrectinib with irinotecan and temozolomide was based on the reported responses to irinotecan and temozolomide in DSRCT (38-41), and that the latter combination.

Acknowledgements

The authors are indebted to the late Dr William Gerald who supervised H.M. in the generation of the Agilent ChIP-chip data used in this paper.

Figure Legends

Figure 1. EWSR1-WT1 binds to the promoter of *NTRK3* and activates its expression.
(A) Overlap of EWSR1-WT1 bound genes identified by ChIP with anti-WT1 and anti-HA antibodies in JN-DSRCT-1 and UF5 cells, respectively, and mining of resulting list for upregulated, potentially targetable genes. (B) Validation of EWSR1-WT1 binding to *NTRK3* promoter by ChIP-qPCR. Each bar represents fold enrichment of peaks relative to non-specific IgG. Error bars represent standard error. The *ASCL1* promoter, a known EWSR1-WT1 target gene, is used as a positive control. *NTRK3* exon 1 and intron 19 are used as negative locus controls (C) Ectopic overexpression of EWSR1-WT1 in HEK293T cells (Western blot, left panel) induces expression of *NTRK3* mRNA but not *NTRK1, NTRK2, or NTF3.* (D) EWSR1-WT1, but not EWS-FLI1, activates luciferase expression driven by the *NTRK3* promoter in HEK293T cells. A western blot probed with HA tag antibody confirmed the expression of the respective fusion proteins (E) *NTRK3* mRNA expression, cell viability, and relative caspase 3/7 activity after siRNA knockdown of *EWSR-WT1* or *WT1*, respectively, in JN-DSRCT-1 and CHP100 Ewing Sarcoma cells. * $P < 0.01$, NS, not significant, student t-test.

Figure 2. NTRK3 is highly expressed in DSRCT.
(A) Average expression of *NTRK3* by sarcoma type based on Affymetrix U133A expression array data on DSRCT and four other translocation sarcomas (ARMS: alveolar rhabdomyosarcoma; ASPS: alveolar soft part sarcoma; ES: Ewing sarcoma; SS: synovial sarcoma). Median is indicated by the horizontal line inside the box and outliers are marked as points. Data were normalized from intensities obtained using the Affymetrix U133A array and show that *NTRK3* expression is higher in DSRCT ($p < 0.001$).
(B) Average expression of *NTRK3* kinase domain based on anchored PCR from Archer-based MSK-Fusion assay data revealed that expression of *NTRK3* is higher in DSRCT cases compared to (non-DSRCT) cases with *NTRK3* fusions ($p < 0.01$, Student's t-test).
(C) Immunohistochemical staining for WT1 NTRK3 in DSRCT tumors. Prominent, diffuse membranous and cytoplasmic staining was seen for NTRK3 in DSRCT cells but not in surrounding stroma. Two representative cases are shown.

Figure 3. *NTRK3* signaling in DSRCT.
qRT-PCR (A) and Western blot (B) confirms high expression of *NTRK3* in and its ligand NTF3 in DSRCT cells, but not in control cells (LP9 and CHP100). NTRK3 is phosphorylated in DSRCT, indicating activation (C). Addition of NTF3 activated phosphorylation of Thr202/Tyr204 of ERK1/2, downstream of NTRK3, in both JN-DSRCT-1 and SK-DSRCT-2 cells (D) and cell growth (E). For growth curves, cells (20,000 cells per well) were seeded in 6-well plates in DMEM:F12 growth medium supplemented with 2% FBS and antibiotics.

Figure 4. Treatment of DSRCT cells with entrectinib and repotrectinib.
Dose-dependent inhibition with entrectinib is demonstrated in JN-DSRCT-1 and SK-DSRCT-2 (IC50; SK-DSRCT-2, 0.95 μM; JN-DSRCT-1, 0.42 μM; LP-9, 2.35 μM; CHP100, 4.78 μM) (A). Target inhibition and downstream signaling following entrectinib treatment in DSRCT cells. Entrectinib inhibits phosphorylation of ERK1/2 in both of the DSRCT cell lines (B). Phosphorylation of NTRK3 is suppressed by entrectinib treatment and activated by NTF3 treatment (C). Dose-dependent curves with repotrectinib are demonstrated in JN-DSRCT-1, SK-DSRCT-2, and CHP100 demonstrated comparable IC_{50} compared with entrectinib in DSRCT (JN-DSRCT-1, 0.29 μM; SK-DSRCT-2, 0.40 μM; CHP100, 1.64 μM) (D). Target inhibition and downstream signaling following repotrectinib treatment in DSRCT cells. Repotrectinib also inhibits phosphorylation of ERK1/2 in both of the DSRCT cell lines: JN-DSRCT-1 and SK-DSRCT-2 (E).

Figure 5. NTRK3 shRNA knockdown.
NTRK3 shRNA knockdown results in loss of NTRK3 expression and reduced cell viability in DSRCT cell lines (A, B) but not in Ewing cell line CHP100 (C). NTRK3 shRNA knockdown decreased phosphorylation of ERK1/2 in DSRCT cells (D). * $P < 0.01$, student t-test.

Figure 6. Entrectinib reduces growth of DSRCT PDX models.
EWSR1-WT1 gene fusion (A, RT-PCR), and *NTRK3* mRNA expression in PDX tumor samples (B). Mice bearing DSRCT PDX tumors were implanted into the subcutaneous flank of Immune compromised mice and treatment began when tumors reached approximately 100-150 mm^3. Mice were treated with vehicle or entrectinib (50 mg/kg, QD, 5 days/week). Area under curve (AUC) was used to compare tumor growth. Pharmacological inhibition of NTRK3 by entrectinib resulted in significantly reduced PDX growth (C-E). Treatment started when tumors reached 80-100 mm3 in volume, which corresponded to day 30 for DSRCT-0027A and DSRCT-0028A, and day 90 for DSRCT-0024B, as indicated by the X axes in panels C to E. In all cases, mice were treated for 6 consecutive weeks, at which time mice were sacrificed and tumors collected for further analysis. Western blot analysis of DSRCT-0027A PDX tumor samples obtained at time of sacrifice confirmed that entrectinib reduced ERK signaling downstream of NTRK3 (F).

Reference

1. Mora J, Modak S, Cheung NK, Meyers P, de Alava E, Kushner B*, et al.* Desmoplastic small round cell tumor 20 years after its discovery. Future Oncol **2015**;11(7):1071-81 doi 10.2217/fon.15.32.
2. Gerald WL, Miller HK, Battifora H, Miettinen M, Silva EG, Rosai J. Intra-abdominal desmoplastic small round-cell tumor. Report of 19 cases of a distinctive type of high-grade polyphenotypic malignancy affecting young individuals. Am J Surg Pathol **1991**;15(6):499-513.
3. Gerald WL, Rosai J. Case 2. Desmoplastic small cell tumor with divergent differentiation. Pediatr Pathol **1989**;9(2):177-83 doi 10.3109/15513818909022347.
4. Shen WP, Towne B, Zadeh TM. Cytogenetic abnormalities in an intraabdominal desmoplastic small cell tumor. Cancer Genet Cytogenet **1992**;64(2):189-91 doi 10.1016/0165-4608(92)90355-c.
5. Ladanyi M, Gerald W. Fusion of the EWS and WT1 genes in the desmoplastic small round cell tumor. Cancer Res **1994**;54(11):2837-40.
6. Gerald WL, Rosai J, Ladanyi M. Characterization of the genomic breakpoint and chimeric transcripts in the EWS-WT1 gene fusion of desmoplastic small round cell tumor. Proc Natl Acad Sci U S A **1995**;92(4):1028-32 doi 10.1073/pnas.92.4.1028.
7. Modak S, Gerald W, Cheung NK. Disialoganglioside GD2 and a novel tumor antigen: potential targets for immunotherapy of desmoplastic small round cell tumor. Med Pediatr Oncol **2002**;39(6):547-51 doi 10.1002/mpo.10151.
8. Lee SB, Kolquist KA, Nichols K, Englert C, Maheswaran S, Ladanyi M*, et al.* The EWS-WT1 translocation product induces PDGFA in desmoplastic small round-cell tumour. Nat Genet **1997**;17(3):309-13 doi 10.1038/ng1197-309.
9. Liu J, Nau MM, Yeh JC, Allegra CJ, Chu E, Wright JJ. Molecular heterogeneity and function of EWS-WT1 fusion transcripts in desmoplastic small round cell tumors. Clin Cancer Res **2000**;6(9):3522-9.
10. Karnieli E, Werner H, Rauscher FJ, 3rd, Benjamin LE, LeRoith D. The IGF-I receptor gene promoter is a molecular target for the Ewing's sarcoma-Wilms' tumor 1 fusion protein. J Biol Chem **1996**;271(32):19304-9 doi 10.1074/jbc.271.32.19304.
11. Kang HJ, Park JH, Chen W, Kang SI, Moroz K, Ladanyi M*, et al.* EWS-WT1 oncoprotein activates neuronal reprogramming factor ASCL1 and promotes neural differentiation. Cancer Res **2014**;74(16):4526-35 doi 10.1158/0008-5472.CAN-13-3663.
12. Liu KX, Collins NB, Greenzang KA, Furutani E, Campbell K, Groves A*, et al.* The use of interval-compressed chemotherapy with the addition of vincristine, irinotecan, and temozolomide for pediatric patients with newly diagnosed desmoplastic small round cell tumor. Pediatric blood & cancer **2020**:e28559 doi 10.1002/pbc.28559.
13. Magnan H, Price A, Chou A, Riedel E, Wexler L, Ambati S*, et al.* A pilot trial of irinotecan, temozolomide and bevacizumab (ITB) for treatment of newly diagnosed patients with desmoplastic small round cell tumor (DSRCT). Journal of clinical oncology : official journal of the American Society of Clinical Oncology **2017**;35(15 suppl):11050.
14. Smith R, Odintsov I, Liu Z, Lui A, Yayashi T, Vojnic M*, et al.* Establishment of multiple novel patient-derived models of desmoplastic small round cell tumor enabling functional characterization of ERBB pathway signaling and pre-clinical evaluation of a novel targeted therapy approach. bioRxiv **2020**;bioRxiv 2020.09.22.308940 doi https://doi.org/10.1101/2020.09.22.308940.
15. Kobos R, Nagai M, Tsuda M, Merl MY, Saito T, Laé M*, et al.* Combining integrated genomics and functional genomics to dissect the biology of a cancer-associated, aberrant transcription factor, the ASPSCR1-TFE3 fusion oncoprotein. J Pathol **2013**;229(5):743-54 doi 10.1002/path.4158.

16. Li H, Smolen GA, Beers LF, Xia L, Gerald W, Wang J*, et al.* Adenosine transporter ENT4 is a direct target of EWS/WT1 translocation product and is highly expressed in desmoplastic small round cell tumor. PLoS One **2008**;3(6):e2353 doi 10.1371/journal.pone.0002353.
17. Kim MS, Yoon SK, Bollig F, Kitagaki J, Hur W, Whye NJ*, et al.* A novel Wilms tumor 1 (WT1) target gene negatively regulates the WNT signaling pathway. J Biol Chem **2010**;285(19):14585-93 doi 10.1074/jbc.M109.094334.
18. Mattar M, McCarthy CR, Kulick AR, Qeriqi B, Guzman S, de Stanchina E. Establishing and Maintaining an Extensive Library of Patient-Derived Xenograft Models. Front Oncol **2018**;8:19 doi 10.3389/fonc.2018.00019.
19. Gerald WL, Ladanyi M, de Alava E, Cuatrecasas M, Kushner BH, LaQuaglia MP*, et al.* Clinical, pathologic, and molecular spectrum of tumors associated with t(11;22)(p13;q12): desmoplastic small round-cell tumor and its variants. Journal of clinical oncology : official journal of the American Society of Clinical Oncology **1998**;16(9):3028-36 doi 10.1200/jco.1998.16.9.3028.
20. Hingorani P, Dinu V, Zhang X, Lei H, Shern JF, Park J*, et al.* Transcriptome analysis of desmoplastic small round cell tumors identifies actionable therapeutic targets: a report from the Children's Oncology Group. Scientific reports **2020**;10(1):12318 doi 10.1038/s41598-020-69015-w.
21. Chakravarty D, Gao J, Phillips SM, Kundra R, Zhang H, Wang J*, et al.* OncoKB: A Precision Oncology Knowledge Base. JCO Precis Oncol **2017**;2017 doi 10.1200/PO.17.00011.
22. Cocco E, Scaltriti M, Drilon A. NTRK fusion-positive cancers and TRK inhibitor therapy. Nat Rev Clin Oncol **2018**;15(12):731-47 doi 10.1038/s41571-018-0113-0.
23. Gedminas JM, Chasse MH, McBrairty M, Beddows I, Kitchen-Goosen SM, Grohar PJ. Desmoplastic small round cell tumor is dependent on the EWS-WT1 transcription factor. Oncogenesis **2020**;9(4):41 doi 10.1038/s41389-020-0224-1.
24. Filion C, Motoi T, Olshen AB, Laé M, Emnett RJ, Gutmann DH*, et al.* The EWSR1/NR4A3 fusion protein of extraskeletal myxoid chondrosarcoma activates the PPARG nuclear receptor gene. J Pathol **2009**;217(1):83-93 doi 10.1002/path.2445.
25. Benayed R, Offin M, Mullaney K, Sukhadia P, Rios K, Desmeules P*, et al.* High Yield of RNA Sequencing for Targetable Kinase Fusions in Lung Adenocarcinomas with No Mitogenic Driver Alteration Detected by DNA Sequencing and Low Tumor Mutation Burden. Clin Cancer Res **2019**;25(15):4712-22 doi 10.1158/1078-0432.CCR-19-0225.
26. Bowman A, Zehir A, Slotkin E, Wexler L, Tap W, Gerstle J*, et al.* MSK-IMPACT GENOMIC PROFILING OF DESMOPLASTIC SMALL ROUND CELL SARCOMA REVEALS RECURRENT COPY NUMBER ALTERATIONS. 2019 November 13-16, 2019; Tokyo, Japan. p 324.
27. Drilon A, Ou SI, Cho BC, Kim DW, Lee J, Lin JJ*, et al.* Repotrectinib (TPX-0005) Is a Next-Generation ROS1/TRK/ALK Inhibitor That Potently Inhibits ROS1/TRK/ALK Solvent- Front Mutations. Cancer discovery **2018**;8(10):1227-36 doi 10.1158/2159-8290.Cd-18-0484.
28. Li XQ, Hisaoka M, Shi DR, Zhu XZ, Hashimoto H. Expression of anaplastic lymphoma kinase in soft tissue tumors: an immunohistochemical and molecular study of 249 cases. Hum Pathol **2004**;35(6):711-21 doi 10.1016/j.humpath.2003.12.004.
29. Saito T, Yokotsuka M, Motoi T, Iwasaki H, Nagao T, Ladanyi M*, et al.* EWS-WT1 Chimeric Protein in Desmoplastic Small Round Cell Tumor is a Potent Transactivator of FGFR4. J Cancer Sci Ther **2012**;4(10):335-40 doi 10.4172/1948-5956.1000164.
30. Akaike K, Suehara Y, Kohsaka S, Hayashi T, Tanabe Y, Kazuno S*, et al.* PPP2R1A regulated by PAX3/FOXO1 fusion contributes to the acquisition of aggressive behavior

in PAX3/FOXO1-positive alveolar rhabdomyosarcoma. Oncotarget **2018**;9(38):25206-15 doi 10.18632/oncotarget.25392.

31. Luo W, Xu C, Ayello J, Dela Cruz F, Rosenblum JM, Lessnick SL*, et al.* Protein phosphatase 1 regulatory subunit 1A in ewing sarcoma tumorigenesis and metastasis. Oncogene **2018**;37(6):798-809 doi 10.1038/onc.2017.378.
32. Tsuda M, Davis IJ, Argani P, Shukla N, McGill GG, Nagai M*, et al.* TFE3 fusions activate MET signaling by transcriptional up-regulation, defining another class of tumors as candidates for therapeutic MET inhibition. Cancer Res **2007**;67(3):919-29 doi 10.1158/0008-5472.Can-06-2855.
33. Ardini E, Menichincheri M, Banfi P, Bosotti R, De Ponti C, Pulci R*, et al.* Entrectinib, a Pan-TRK, ROS1, and ALK Inhibitor with Activity in Multiple Molecularly Defined Cancer Indications. Mol Cancer Ther **2016**;15(4):628-39 doi 10.1158/1535-7163.Mct-15-0758.
34. Lee SJ, Li GG, Kim ST, Hong ME, Jang J, Yoon N*, et al.* NTRK1 rearrangement in colorectal cancer patients: evidence for actionable target using patient-derived tumor cell line. Oncotarget **2015**;6(36):39028-35 doi 10.18632/oncotarget.5494.
35. Russo M, Misale S, Wei G, Siravegna G, Crisafulli G, Lazzari L*, et al.* Acquired Resistance to the TRK Inhibitor Entrectinib in Colorectal Cancer. Cancer Discov **2016**;6(1):36-44 doi 10.1158/2159-8290.Cd-15-0940.
36. Smith KM, Fagan PC, Pomari E, Germano G, Frasson C, Walsh C*, et al.* Antitumor Activity of Entrectinib, a Pan-TRK, ROS1, and ALK Inhibitor, in ETV6-NTRK3-Positive Acute Myeloid Leukemia. Mol Cancer Ther **2018**;17(2):455-63 doi 10.1158/1535-7163.Mct-17-0419.
37. Drilon A, Siena S, Ou SI, Patel M, Ahn MJ, Lee J*, et al.* Safety and Antitumor Activity of the Multitargeted Pan-TRK, ROS1, and ALK Inhibitor Entrectinib: Combined Results from Two Phase I Trials (ALKA-372-001 and STARTRK-1). Cancer Discov **2017**;7(4):400-9 doi 10.1158/2159-8290.Cd-16-1237.
38. Aguilera D, Hayes-Jordan A, Anderson P, Woo S, Pearson M, Green H. Outpatient and home chemotherapy with novel local control strategies in desmoplastic small round cell tumor. Sarcoma **2008**;2008:261589 doi 10.1155/2008/261589.
39. Angarita FA, Hassan S, Cannell AJ, Dickson BC, Gladdy RA, Swallow CJ*, et al.* Clinical features and outcomes of 20 patients with abdominopelvic desmoplastic small round cell tumor. European journal of surgical oncology : the journal of the European Society of Surgical Oncology and the British Association of Surgical Oncology **2017**;43(2):423-31 doi 10.1016/j.ejso.2016.08.017.
40. Pinnix CC, Fontanilla HP, Hayes-Jordan A, Subbiah V, Bilton SD, Chang EL*, et al.* Whole abdominopelvic intensity-modulated radiation therapy for desmoplastic small round cell tumor after surgery. International journal of radiation oncology, biology, physics **2012**;83(1):317-26 doi 10.1016/j.ijrobp.2011.06.1985.
41. Rosoff PM, Bayliff S. Successful clinical response to irinotecan in desmoplastic round blue cell tumor. Medical and pediatric oncology **1999**;33(5):500-3 doi 10.1002/(sici)1096-911x(199911)33:5<500::aid-mpo12>3.0.co;2-x.

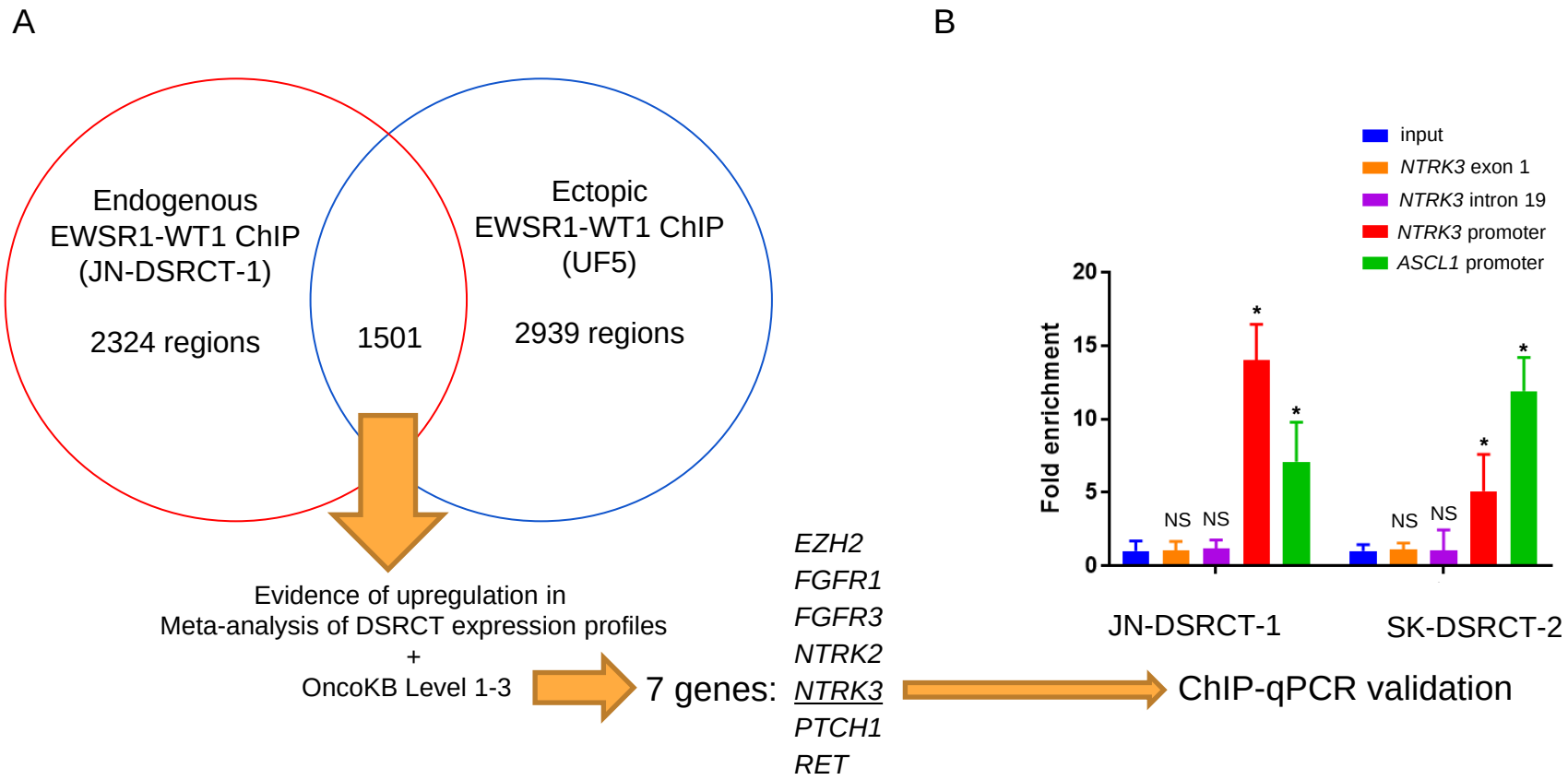

Figure 1. Identification of *NTRK3* as a potentially actionable direct target of EWSR1-WT1.

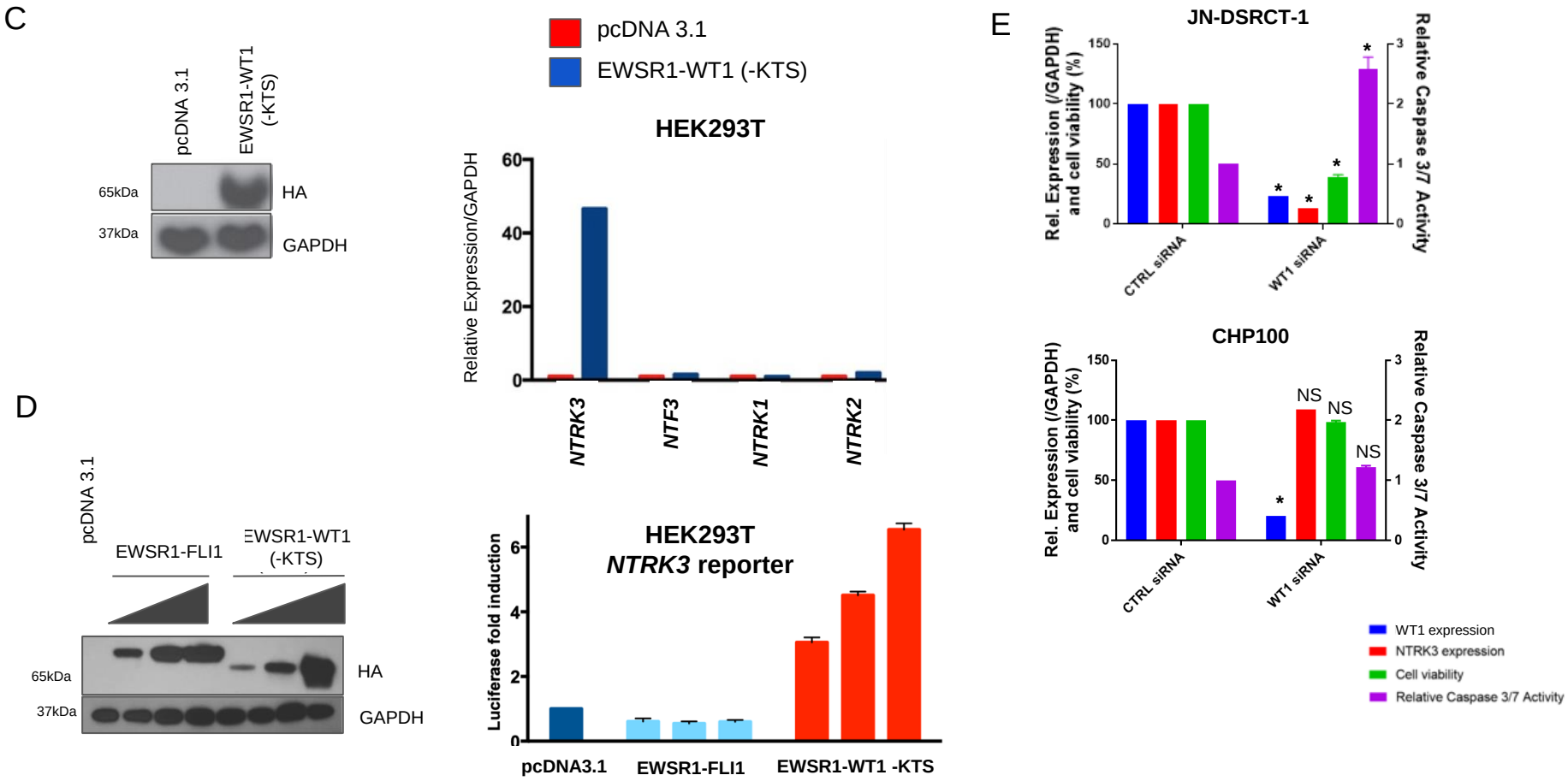

Figure 1.

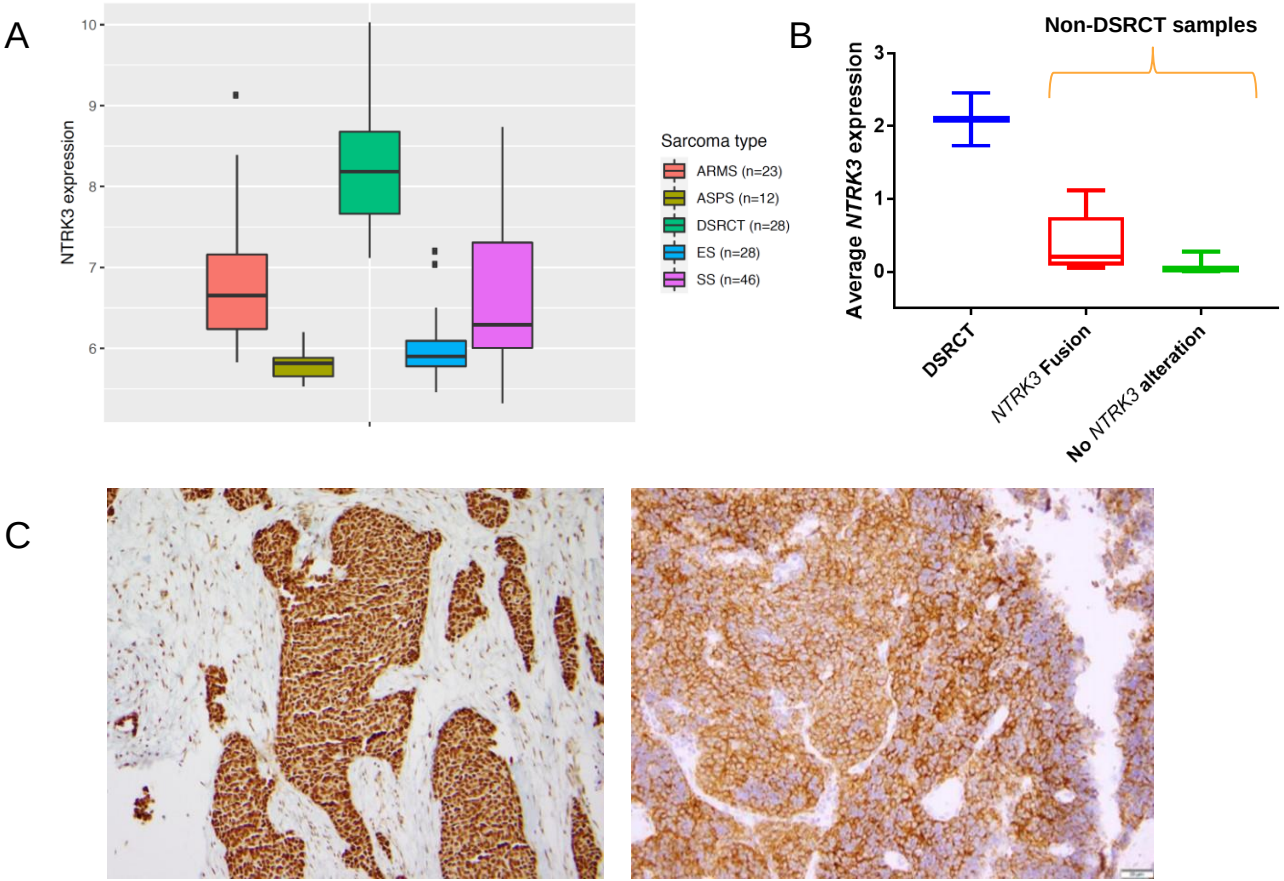

Figure 2. NTRK3 is highly expressed in DSRCT.

Figure 3. *NTRK3* signaling in DSRCT.

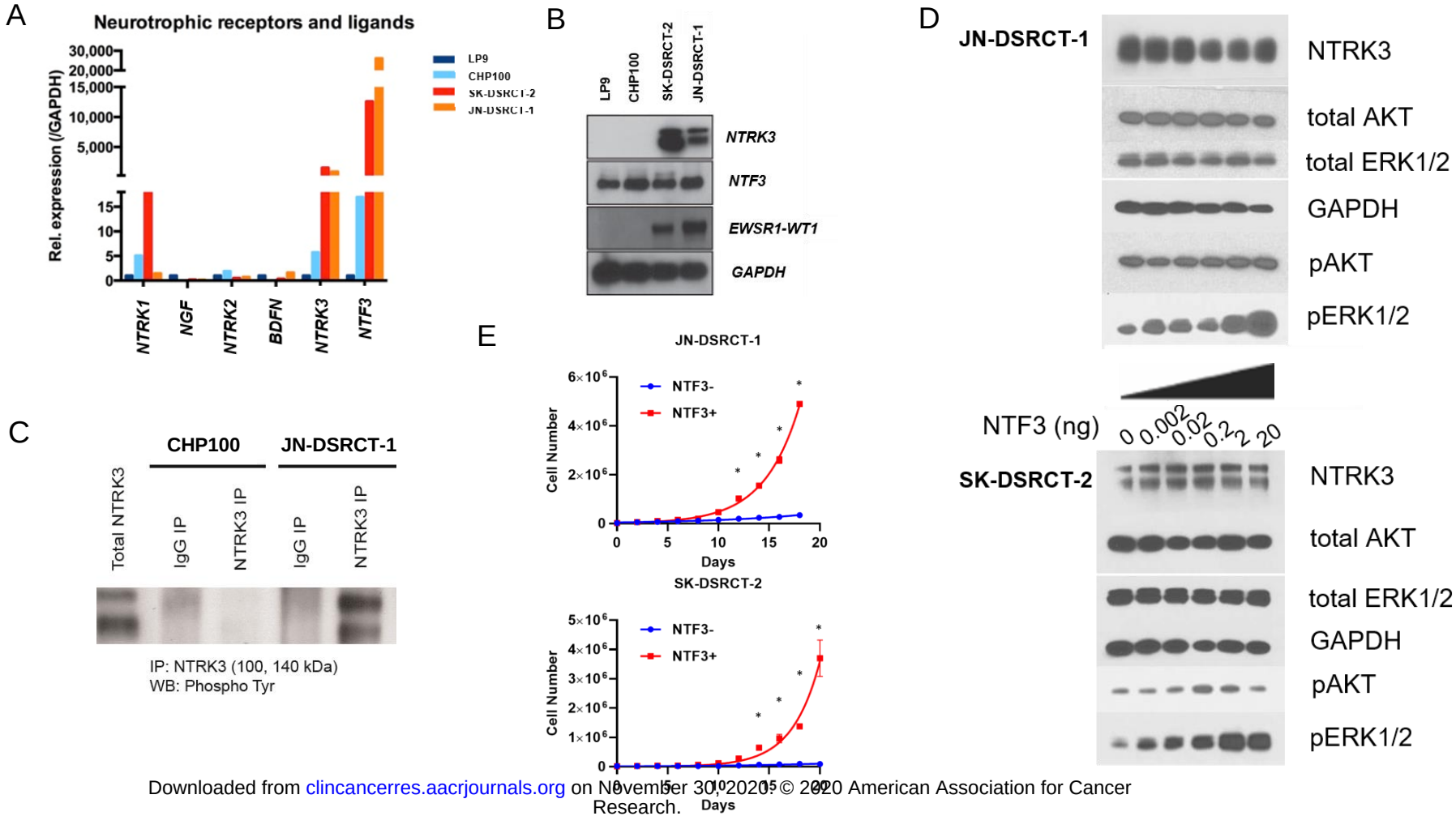

Figure 4. Treatment of DSRCT cells with entrectinib and repotrectinib.

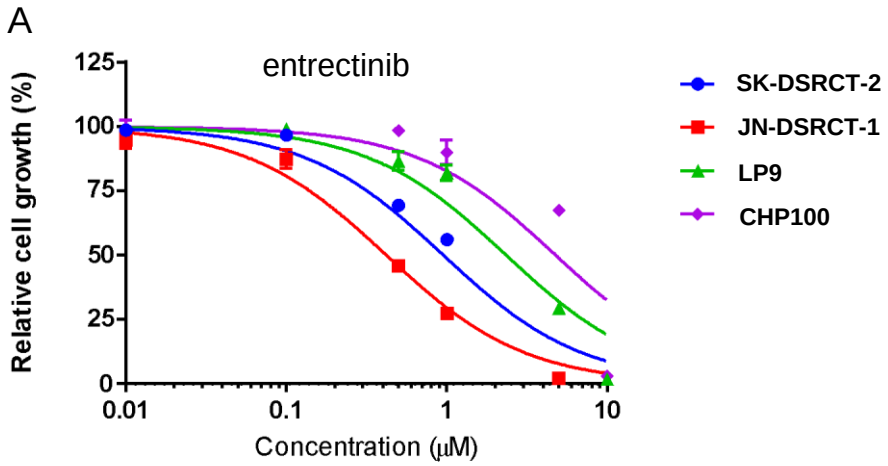

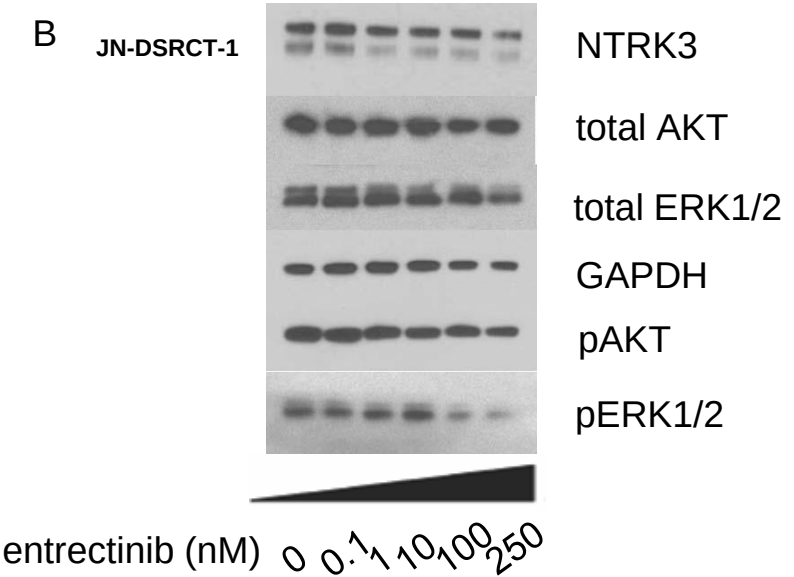

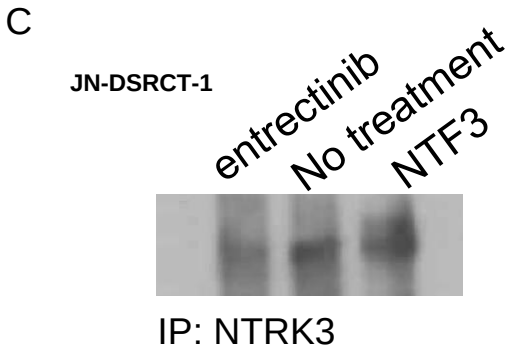

D

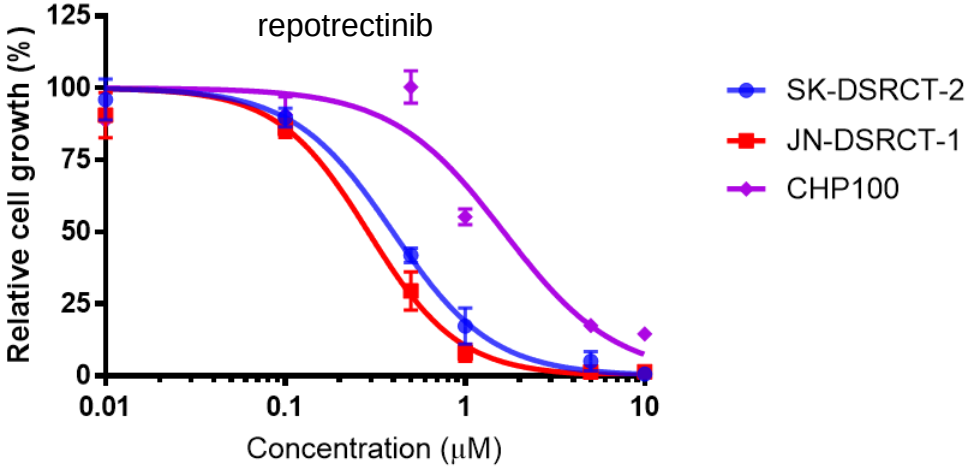

E

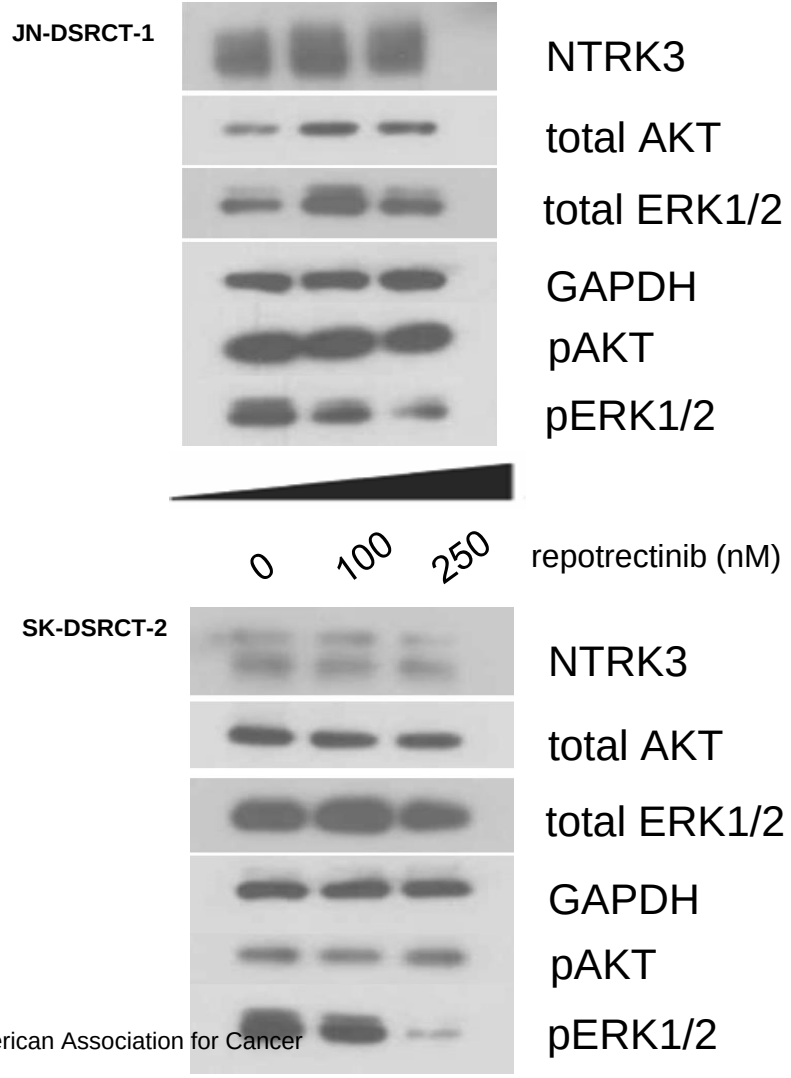

Figure 4.

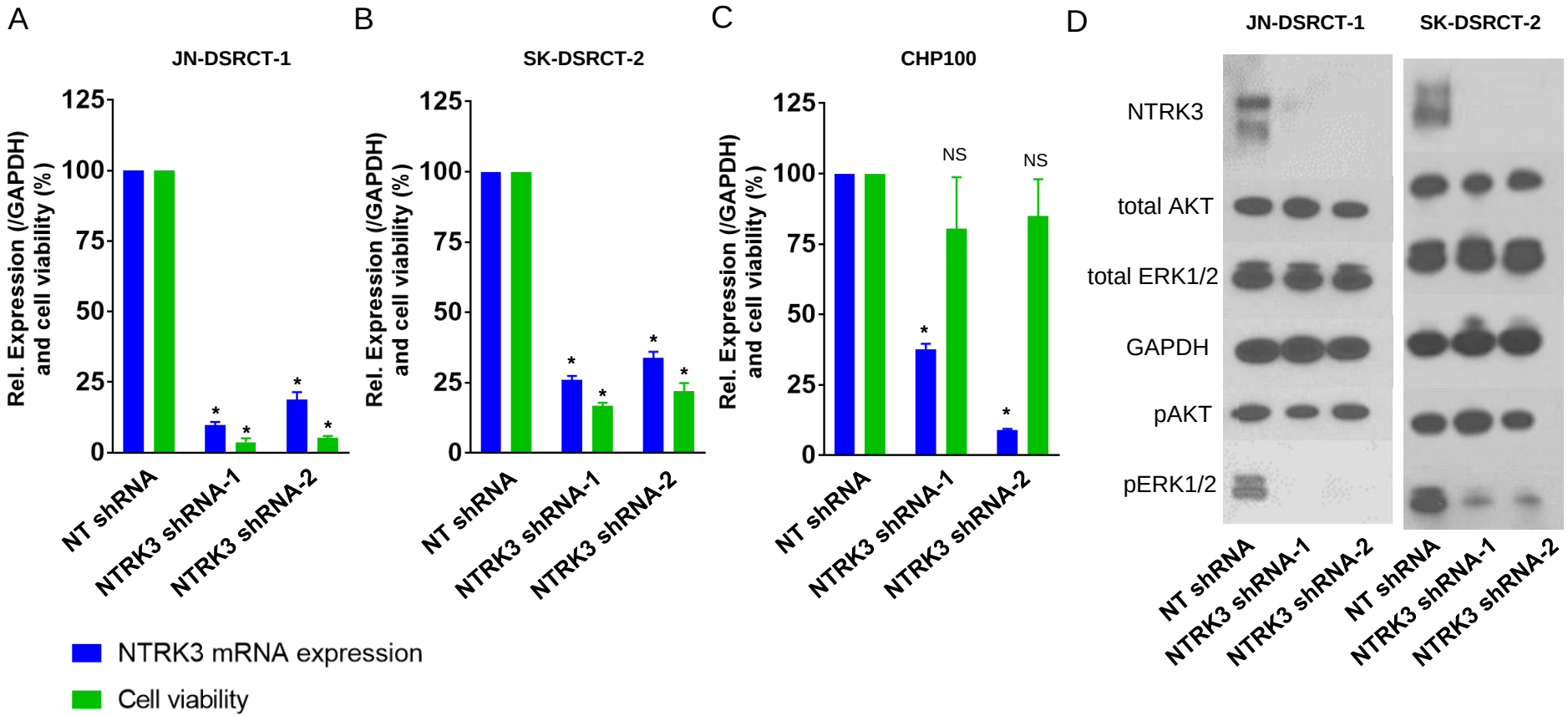

Figure 5. NTRK3 shRNA knockdown.

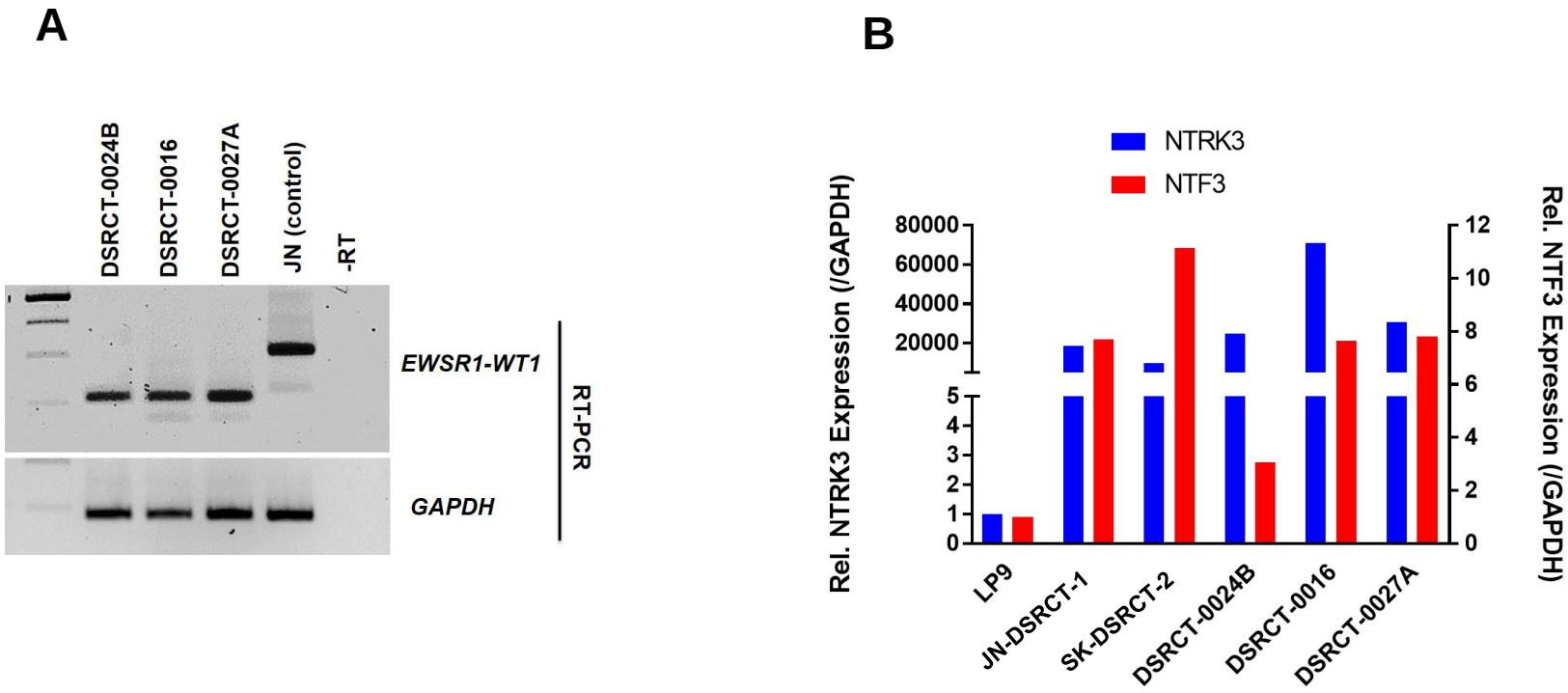

Figure 6. Entrectinib reduces growth of DSRCT PDX models.

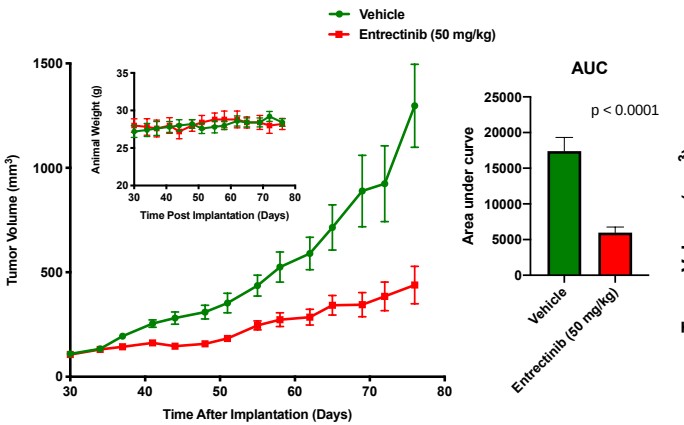

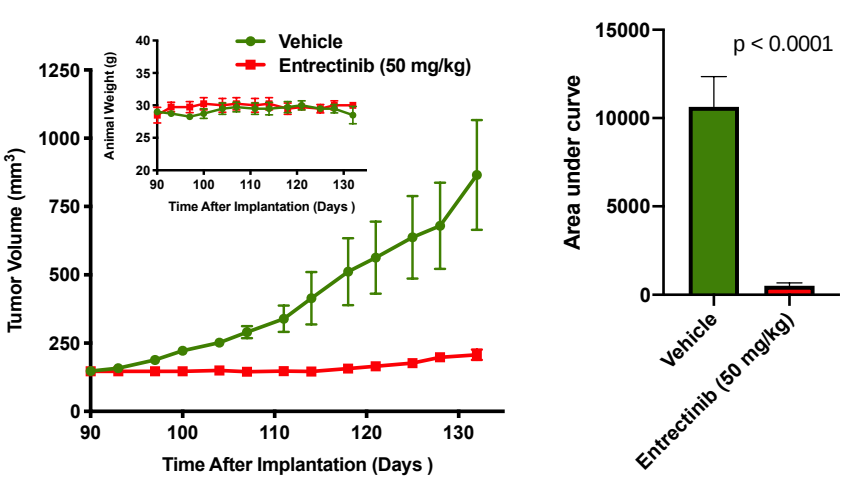

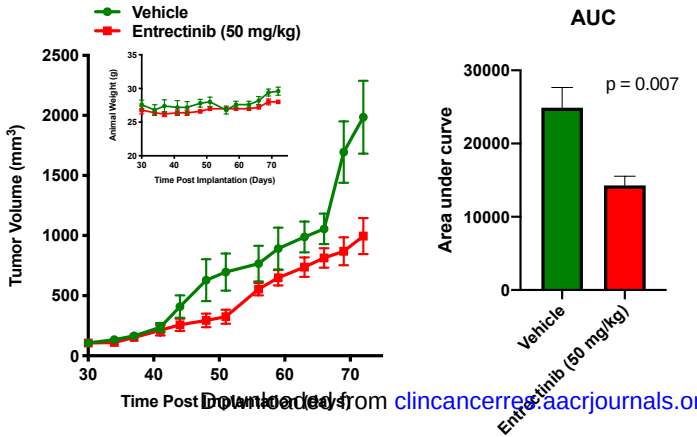

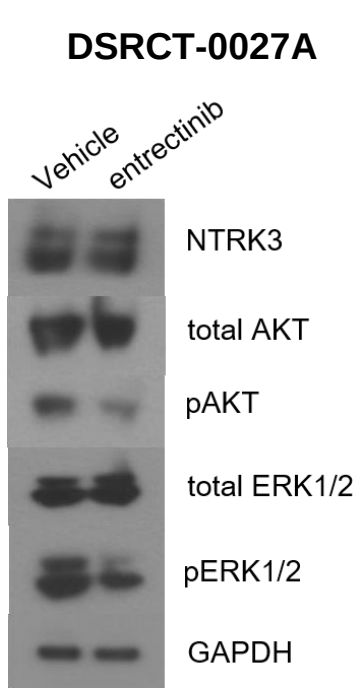

Figure 6.

AACR American Association for Cancer Research

Clinical Cancer Research

Therapeutic potential of NTRK3 inhibition in desmoplastic small round cell tumor

Koichi Ogura, Romel Somwar, Julija Hmeljak, et al.

Clin Cancer Res Published OnlineFirst November 23, 2020.